Evaluation of Safety Margins in the Seismic Design Analysis of a Fast Reactor Core

Massimo Forni, Maurizio Indirli, Alessandro Martelli, Roberto Orsi
ENEA, Bologna, Italy

INTRODUCTION

Seismic design analysis of liquid metal fast reactor (LMR) cores is usually performed taking into account the non-linear effects of shocks occurring among the core elements and the effects of vessel-core mechanical coupling. For the existing reactors, however, the dynamic runs were carried out using one-dimensional (1D) codes and mainly limiting the analysis to the core diameters. Furthermore, simplified approaches were adopted to account for the fluid effects: these neglect the non-diagonal added mass terms (Martelli et al, 1987a).

Thus, an improved methodology has been developed. Its main features are presented below, together with the results of application to the PEC fast reactor core at Safe-Shutdown Earthquake (SSE) and comparison with the design data.

MAIN FEATURES AND RESULTS OF PEC CORE DESIGN ANALYSIS AT SSE

The design calculations of the PEC core (Martelli et al, 1987a) were performed using the 1D computer code CORALIE (Martelli et al, 1981). The in-air natural frequencies of the core elements had been derived from the data obtained for complete full-scale mock-ups, tested at relatively low excitations. The diagonal terms of the added mass matrix had been obtained from the experimental results of other core geometries. They provided a decrease of 20% of the in-air first natural frequency of each element (the non-diagonal terms of such matrix were neglected). Finally, 5% damping was assumed for all the elements, to compensate the conservative nature of the fluid model used (Fig. 1).

Figs. 2-4 report the maximum values of the shock forces and displacements of the various element types, which were computed at SSE in the case that the PEC test channel is replaced by a group of seven elements (this is the geometry assumed in our study). These figures also contain the values used in the structural verifications.

Furthermore, Fig. 5 shows the computed reactivity insertion peaks (the reactivity insertion time-histories were later conservatively normalized to the value corresponding to core geometric radial compaction, for evaluating the neutronic and thermal effects of SSE). Finally, Fig. 6 presents the transfer functions calculated between the diagrid accelerations and the mechanical reaction loads transmitted by the core to the vessel through the diagrid and core-restraint ring.

MAIN FEATURES OF THE IMPROVED METHODOLOGY AND ANALYSIS

Improved natural frequency and damping values of the core elements have been adopted with respect to the design analysis (Fig. 1). They were obtained basing on the results of shake table tests of element prototypes in water, performed with excitation increasing up to above SSE (Martelli et al, 1987b).

Furthermore, the analysis has accounted for the effects of the non-diagonal terms of the added mass matrix on the seismic loads acting at core diagrid. Because it had been demonstrated that fluid coupling among the core elements is negligible compared to that existing between vessel and core (Martelli et al, 1987b, Forni et al, 1988, and Zaniboni, 1989), the mentioned loads have been set equal to the quantities $[-(m'_e+m'_{eD}-m'_{eND})\cdot A(t)]$, in which A is the diagrid acceleration during time t, m'_e are the actual linear element masses, and m'_{eD} and m'_{eND} are the values per unit length of the diagonal and respectively, non-diagonal terms of the added mass matrix related to vessel-core coupling.

In the core motion equations, however, the terms $[m'_{eND}\cdot a_v(t)]$, which are related to the fluid coupling caused by vessel accelera - tion relative to the diagrid (a_v), have been neglected, due to the high wall stiffnesses of the vessel and internal shields: this made it possible to determine the core response separately from that of the other reactor-block components (Forni et al, 1989).

The m'_{eD}- and m'_{eND}- values have been computed by uniformly splitting on the core elements those (m'_{cD} and m'_{ND}) obtained for the vessel - core system by use of the model valid in the case of two shells separated by the liquid. In this model, the outer radius (R_2) is that of the most interior shield which surrounds the core.

As far as the inner radius (R_1) is concerned, the value (R_{1e}) of the shell whose area is equal to that of the core has been used in the factors which account for the finite sizes of the fluid medium (Zaniboni, 1989). On the contrary, the core hydraulic radius (R_{1h}) has usually been adopted in the asymptotic added mass terms which correspond to the case of an infinite fluid medium between the two shells (Martelli et al, 1987b, Forni et al, 1988, and Zaniboni, 1989). (Some runs have also been performed assuming $R_1=R_{1e}$ even in the latter terms, in order to analyse the sensitivity of core response to different fluid models).

The diagonal added mass term related to the vessel (m'_{vD}) has been evaluated by use of the fluid mass balance (Forni et al, 1989). It has been attached to the most interior shield located inside the vessel, at the center of gravity of this shield.

The analysis has also accounted for the coupling loads transmitted by the core to the vessel through the fluid. More precisely, that part of the loads, transmitted by the core to the vessel through the fluid, which is related to the coupling terms $[m'_{ND}\cdot a_c(t)]$ (a_c = core acceleration relative to the diagrid), has been combined with the mechanical reaction loads of the core, while the effects of the remaining part of these loads $[m'_{ND}\cdot A(t)]$ have been taken into account by subtracting m'_{ND} from the mass attached to the most interior shield at the center of gravity: this shield is very stiff and vessel first natural frequency is governed by the relatively low stiffness of its supporting structure (Forni et al, 1989).

The vessel-core interactions due to fluid and mechanical coupling have been determined through an iterative procedure similar to that used in the design analysis. This procedure has involved linear calculations of the entire reactor-block and non-linear CORALIE runs of the core, limited to its diameter in the direction normal to hexcan faces (face-to-face, or X, direction). The difference with respect to the design method is that the linear core models adopted in the reactor-block calculations (which are assessed basing on the transfer functions calculated between the diagrid acceleration and the core reaction loads) have also accounted for the mentioned parts of the vessel-core fluid coupling loads (the linear core mass was $[m'_C+m'_{CD}-m'_{ND}]$). The iterative procedure has been applied to both the initial (INI) and most fanned-out (MFO) core conditions during reactor life (Fig. 6 shows that the two different core geometries affect vessel-core coupling in a diffe - rent way, contrary to the results obtained in the design analysis).

After convergence of this procedure, displacements and reactivity insertion peaks have also been computed by means of two-dimensional (2D) runs of the whole core with the CLASH program (Preumont et al, 1987). These runs have been performed with both 1D and 2D simultaneous excitations, normal to one another (X and corner-to-corner, or Y, directions), for both the initial and most fanned-out core conditions. For the inner elements, they have made use of the shock stiffness values which correspond to the static contact map of the core (k^+_{sh}), according to high core compaction at SSE.

On the contrary, the CORALIE calculations had mainly been based on lower values, obtained experimentally in the case of equal simultaneous loading of two opposite faces (k_{sh}), in order to compute shock force data consistent with those used in the structural and functional verifications of the shrouds (Martelli et al, 1987a): only after convergence of the iterative procedure one CORALIE run has been carried out by use of the k^+_{sh}'s for both core geometries, in order to assess displacements, and especially, reactivity insertion (it has been found that shock stiffnesses do not affect the linear core model features, see Fig. 6).

No further steps of the iterative procedure (by use of CLASH runs) have been necessary, because the method assessed to extrapolate the reaction loads computed in the single row analysis, to the whole core (Martelli et al, 1987a), has been found correct (Fig. 6).

RESULTS OF THE STUDY

Figs. 2-4 show that the maximum displacements and shock forces computed in the PEC design analysis are adequate. However, the margins are frequently not large (in spite of some rather conservative assumptions made in such analysis, especially with regard to the fluid effects). Furthermore, the effects of the different assumptions concerning R_1 are small, in spite of the large effects on the linear core model features (Fig. 6).

With regard to reactivity insertion (Fig. 5), while the peaks computed with CORALIE are only slightly larger than those determined in the design analysis, the CLASH values are rather larger, especially in the most fanned-out core conditions (by 50% in the case of 2D excitation). However, the maximum reactivity value obtained (371 pcm = 0.9 $) is only slightly larger than that corresponding to geometric radial compaction (356 pcm). This confirms that full compaction of the fuel elements occurs at SSE (the above-mentioned slight difference is due to some hexcan deformation). By adding the small vertical effect, i.e. 10 pcm (Martelli et al, 1987a), the total reactivity peak is still lower than the dollar (410 pcm).

CONCLUSIONS

The main features of an improved method for the analysis of the LMR core seismic response have been outlined. It has been clarified how this method accounts for the fluid coupling existing between core and vessel, and for both the 2D nature of core response and the 2D features of horizontal excitation. An example of application, based on the PEC data, has been presented.

It has been shown that 1D analysis, limited to core face-to-face diameters, is adequate to evaluate vessel-core coupling effects. Thus, a few 2D runs are sufficient. These runs are necessary to account for the 2D effects, the effects of interactions between the core diameter and the other adjacent element rows, as well as the possibility that maximum response occurs outside the diameter. Moreovever, these runs are particularly important to evaluate reactivity effects, which look largely underestimated by 1D analysis.

With regard to the comparison with the results of the PEC design analysis, it has been found that these are adequate, but the margins are frequently not large. For this reason and considering that the features of the improved method are not such as to complicate the analysis too much, the authors believe that seismic design of the future LMR cores should be performed by use of methods similar to that adopted in this study.

REFERENCES

Forni , M. , Martelli , A. , Melloni , R. and Bonacina , G. (1988). Detailed Comparison between Computed and Measured FBR Core Seismic Responses. Proc. 6th ASME - PVP Conf., Pittsburgh, PA, USA, PVP-Vol. 145, pp. 1-18.

Forni , M. , Indirli , M. , Martelli , A. and Orsi , R. (1989). An Improved Method for the LMR Core Seismic Analysis and Compari - son with the Usual Design Approaches. Proc. Intl. Symposium on Pressure Vessel Technology and Nuclear Codes and Standards , Seoul, Korea.

Martelli , A. , Gauvain , J. and Bernard , A. (1981). Non - Linear Dynamic and Seismic Analysis of Fast Reactor Cores. Proc. 6th Intl. SMiRT Conf., Paris, France, Vol. K(b) , pp. 1-8.

Martelli, A. , Forni, M., Micelotta, A., Sartori, C. and Bonacina , G. (1987a). PEC Fast Reactor Core Seismic Verification. Proc. 9th Intl. SMiRT Conf., Lausanne, Switzerland, Vol.E, pp. 15-26.

Martelli, A., Forni, M., Micelotta A., Paoluzzi, R., Bonacina , G. and Melloni , R. (1987b) . Evaluation of Fluid Effects on the Dynamic Response of a Fast Reactor Core. Proc. 5th ASME - PVP Conf., Pittsburgh, PA, USA, PVP-Vol. 128, pp. 1-30.

Preumont, A., Pay, A. and Decauwers, A. (1987). Seismic Analysis of a Large FBR Core. Some SNR-2 Preliminary Calculations. Proc. 9th Intl. SMiRT Conf., Lausanne, Switzerland, Vol.E, pp. 27-32.

Zaniboni, E. (1989). Analisi della Risposta Sismica Sperimentale di Modelli di Nocciolo di Reattori Refrigerati a Metallo Liquido . Master Thesis, University of Bologna, Italy.

Element type	1st natural frequency $R_1 = R_{1h}$	1st natural frequency $R_1 = R_{1e}$	1st natural frequency design anal.	2nd natural frequency $R_1 = R_{1h}$	2nd natural frequency $R_1 = R_{1e}$	2nd natural frequency design anal.	damping this work	damping design
ECD	2.78	2.43	2.86	20.0	17.4	21.6	2.0%	5%
ES	3.19	2.70	2.92	24.8	21.0	27.5	1.5%	5%
ERN	2.99	2.68	2.63	21.9	19.6	19.6	1.5%	5%
ECP	2.78	2.43	2.86	20.0	17.4	21.6	2.0%	5%
ERF	2.88	2.58	2.88	21.6	19.3	20.2	1.0%	5%
ECC	2.79	2.44	2.94	20.0	17.4	21.8	2.0%	5%

Fig. 1 : First and second natural frequencies [Hz] and fractions of critical damping , compared to the values of the design analysis . ECD = elements in decay positions; ES = neutron shield elements ; ERN = normal reflecting elements ; ECP = forced-type fuel elements; ERF = forced reflecting elements ; ECC = normal-type fuel elements.

Element type	axial level [mm]	INI core R_{1e} k_{sh}	INI core R_{1h} k_{sh}	INI core des. k_{sh}	INI core ver. k_{sh}	MFO core R_{1h} k_{sh}	MFO core des. k_{sh}	MFO core ver. k_{sh}	margins INI core	margins MFO core
ECC	1440	175	247	198	370	272	438	440	50%	62%
	2558	427	463	468	1120	515	528	1240	142%	141%
ERF	1440	203	297	240	370	282	405	440	25%	56%
	2558	467	497	470	590	562	514	820	19%	46%
ECP	1440	231	237	254	370	266	403	440	56%	65%
	2558	561	614	580	1120	742	727	1240	82%	67%
EBC	1440	231	237	254	370	266	403	440	56%	65%
	2558	570	577	580	580	638	727	730	1%	14%
ERN	1440	255	246	366	370	235	294	440	45%	87%
	2558	561	544	588	590	721	821	820	5%	14%
ES	1440	326	250	426	710	382	447	910	118%	138%
	2558	646	587	707	710	854	913	910	10%	7%
ECD	1440	88	163	342	370	206	375	440	127%	114%
	2558	1067	1050	1124	1120	1130	1237	1240	5%	10%

Fig. 3 : Maximum shock forces [daN] computed at both pads levels. Comparison with the single design values and those consistent with the methodology adopted for shroud verifications.

Element type	initial core (INI) R_{1e} k_{sh}	initial core (INI) R_{1h} k_{sh}	initial core (INI) R_{1h} k_{sh}+	initial core (INI) des. k_{sh}	initial core (INI) ver. k_{sh}	fanned-out core (MFO) R_{1h} k_{sh}	fanned-out core (MFO) R_{1h} k_{sh}+	fanned-out core (MFO) des. k_{sh}	fanned-out core (MFO) ver. k_{sh}
ECC	23.6	23.1	22.1	23.1	26	25.0	23.2	24.0	26
ERF	23.9	23.4	22.4	23.5	27	25.4	23.5	24.4	27
ECP	24.4	24.4	24.1	25.6	26	26.6	26.7	26.3	26
EBC	24.4	24.4	24.1	25.6	26	26.6	26.7	26.3	26
ERN	23.7	23.9	23.8	27.3	27	24.7	25.1	26.9	27
ES	18.0	18.8	21.5	25.5	25	18.7	20.2	25.0	25
ECD	15.5	16.5	18.2	26.3	26	17.2	19.2	26.2	26

Fig. 2 : Maximum displacements [mm] calculated at upper pads. Comparison with the single design values and those consistent with the methodology adopted for the spike verifications.

Element type	CORALIE diam.	CLASH 1D diam.	CLASH 1D core	CLASH 2D diam.	CLASH 2D core	design anal.	spike verific.	margins of the verif.	
ECC	22.1	25.4	25.4	25.9	25.9	29	34	31%	INI
ERF	24.4	26.1	27.1	26.7	27.8	30	32	15%	
ECP	24.1	26.3	26.8	26.4	27.2	30	34	25%	
EBC	24.1	26.3	26.8	26.4	27.2	30	31	14%	
ERN	23.8	26.6	26.9	24.8	27.8	32	32	15%	
ES	21.1	20.3	23.8	20.3	23.8	25	36	51%	
ECD	18.2	16.9	17.1	16.6	19.8	22	34	72%	
ECC	23.2	28.3	28.3	27.6	27.6	29	34	20%	MFO
ERF	23.5	28.9	30.1	28.3	30.3	30	32	6%	
ECP	26.7	29.5	30.7	28.4	30.4	30	34	11%	
EBC	26.7	29.5	30.7	28.2	29.9	30	31	1%	
ERN	25.1	27.8	28.6	26.9	29.1	32	32	10%	
ES	20.2	21.7	26.5	22.2	24.4	25	36	36%	
EDC	19.2	17.4	17.9	17.7	20.7	22	34	64%	

Fig. 4 : Maximum displacements [mm] calculated with CLASH at upper pad level on the diameter and the whole core in the initial (INI) and the most fanned-out (MFO) core conditions, with 1D and 2D excitations. Comparison with the CORALIE results, the design values and those used for the spike verifications.

core conditions	design analysis CORALIE	improved analysis CORALIE	improved analysis CLASH 1D	improved analysis CLASH 2D
initial	0.38	0.38	0.47	0.41
most fanned-out	0.60	0.64	0.83	0.90

Fig. 5 : Comparison between the reactivity insertion peaks computed with CLASH and CORALIE [dollars]. Comparison with the design values

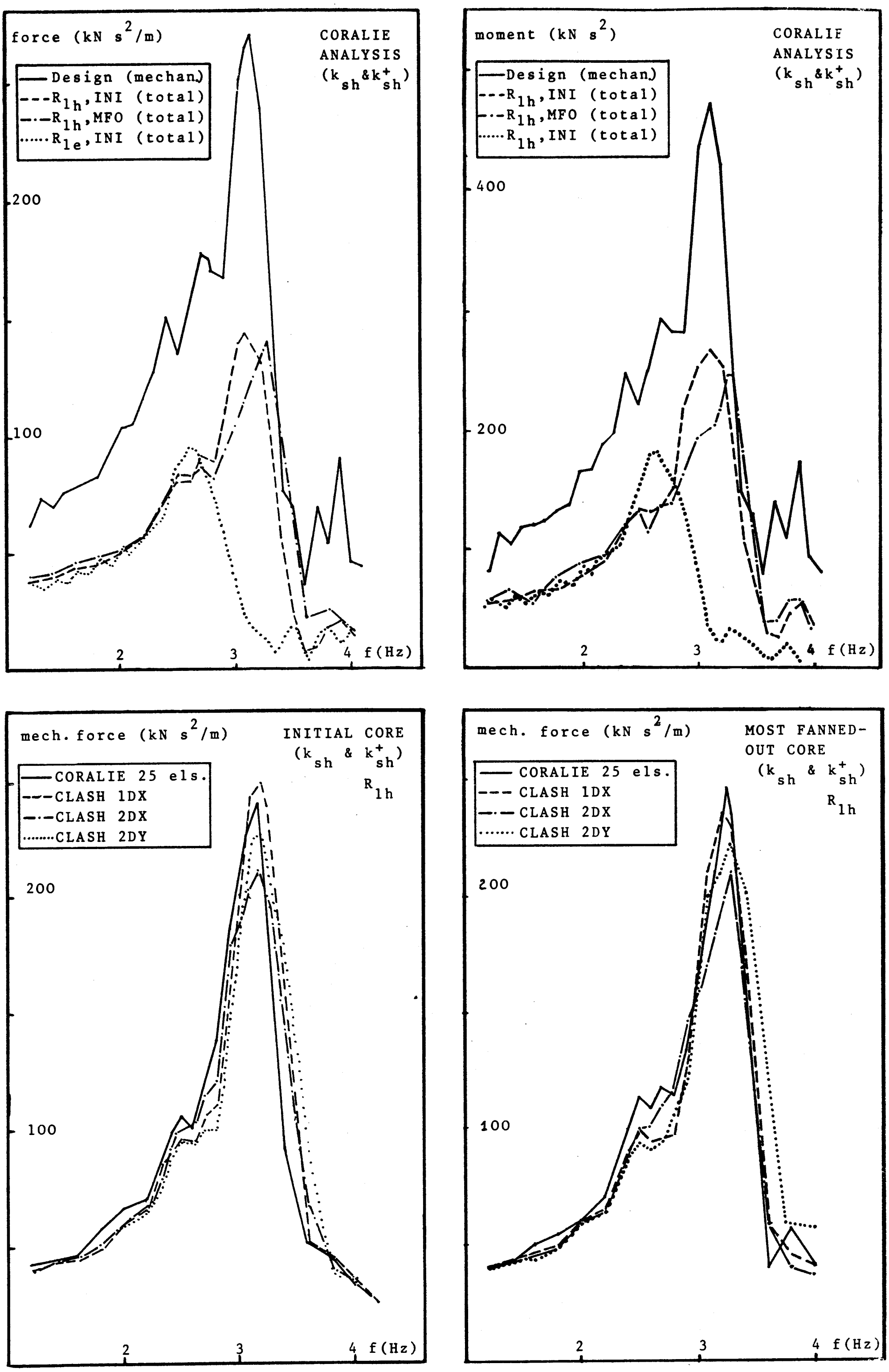

Fig. 6 : Transfer functions between diagrid acceleration and core reaction loads.